Boundary-Layer Meteorol (2008) 129:47–64
DOI 10.1007/s10546-008-9309-7

ORIGINAL PAPER

A Flume Experiment on the Adjustment of the Mean and Turbulent Statistics to a Transition from Short to Tall Sparse Canopies

Anthony Seraphin · Philippe Guyenne

Received: 10 May 2007 / Accepted: 21 August 2008 / Published online: 13 September 2008

Abstract Water-flume experiments are conducted to study the structure of turbulent flow within and above a sparse model canopy consisting of two rigid canopies of different heights. This difference in height specifies a two-dimensional step change from a rough to a rougher surface, as opposed to a smooth-to-rough transition. Despite the fact that the flow is in transition from a rough to a rougher surface, the thickness of the internal boundary layer scales as $x^{4/5}$, consistent with smooth-to-rough boundary layer adjustment studies, where x is the downstream distance from the step change. However, the analogy with smooth-to-rough transitions no longer holds when the flow inside the canopy and near the canopy top is considered. Results show that the step change in surface roughness significantly increases turbulence intensities and shear stress. In particular, there is an adjustment of the mean horizontal velocity and shear stress as the flow passes over the rougher canopy, so that their vertical profiles adjust to give maximum values at the top of this canopy. We also observe that the magnitude and shape of the inflection in the mean horizontal velocity profile is significantly affected by the transition. The horizontal and vertical turbulence spectra compare well with Kolmogorov's theory, although a small deviation at high frequencies is observed in the horizontal spectrum within the canopy. Here, for relatively low leaf area index, shear is found to be a more effective mechanism for momentum transfer through the canopy structure than vortex shedding.

Keywords Boundary layer · Canopy turbulence · Roughness change · Water flume

A. Seraphin
Department of Mathematical Sciences and Center for Climatic Research, University of Delaware, Newark, DE 19716, USA

P. Guyenne (✉)
Department of Mathematical Sciences, University of Delaware, 501 Ewing Hall, Newark, DE 19716-2553, USA
e-mail: guyenne@math.udel.edu

1 Introduction

Boundary-layer turbulence plays a central role in transferring mass, momentum and energy between the land surface and the atmosphere. Over the last three decades, much progress has been made in understanding the nature of turbulent flows within and above plant canopies, based on experimental data collected from wind-tunnel and field experiments (e.g. Shaw et al. 1974a; Brunet et al. 1994; Poggi et al. 2004b; Zhu et al. 2006). These typically show that mean velocity profiles exhibit an inflection point at canopy height, which suggests that canopy flows are subject to the Kelvin–Helmholtz instability and thus are more similar to mixing layers than rough-wall boundary layers. This yields the picture that turbulence in the vicinity of vegetation canopies is to a large extent dominated by intermittent and energetic coherent structures, whose length scales are of the order of canopy height (Raupach et al. 1996; Finnigan 2000).

Because much research has focused on cases of uniform canopies, attention is now directed to more realistic situations such as canopies on topography (e.g. on hills, with windbreaks and near clearings or edges), and canopies with sparse or non-uniform vegetation. Wind-tunnel experiments were conducted by e.g. Finnigan and Brunet (1995) for a tall canopy on a hill, Judd et al. (1996) for a canopy with multiple windbreaks, and Morse et al. (2002) for the transition from open moorland to a forest. Field studies have also been done of flow over forest edges by e.g. Bergen (1975); Irvine et al. (1997), and Flesch and Wilson (1999). More recent works include Belcher et al. (2003) who developed a model to analyse the adjustment of a turbulent boundary layer to a canopy of roughness elements, Poggi et al. (2004b) who examined the effect of vegetation density on canopy sub-layer turbulence, as well as large-eddy simulations by Yang et al. (2006a, b); Cassiani et al. (2008), and Dupont and Brunet (2008) for turbulent flows across forest edges. We also note the recent works by Ghisalberti and Nepf (2006) who investigated the structure of the shear layer in flows over submerged aquatic vegetation, and by Py et al. (2006) who modelled the interaction between wind and crop canopies. These two studies examined in particular the waving motion of flexible plant canopies in response to the passage of coherent structures generated by Kelvin–Helmholtz instability, and their effects on boundary-layer dynamics.

Following this line of investigation, the present paper presents an experimental study to analyse the changes to a flow as it passes over a sparse, inhomogeneous canopy. Water-flume experiments are carried out using two rigid canopies of different heights to specify a two-dimensional step change in surface roughness. Of special interest here is the transition from a rough to a rougher surface, as opposed to a smooth-to-rough transition in experiments with a single uniform canopy. The structure of the turbulent velocity field, as well as the evolution and geometry of the resulting boundary layer, are investigated in detail.

Our primary goal is to evaluate the effects of an abrupt change in surface roughness on the nature of the flow within and above a model canopy. To do so, a number of boundary-layer characteristics are measured, including (1) mean velocity profiles at several stations downstream from the leading edge of the model canopy, along its central axis, (2) turbulence intensity variations, (3) turbulence spectra within and above the model canopy, (4) turbulent shear stress, (5) correlation coefficient for turbulent shear stress, (6) intermittent events, and (7) growth of the internal boundary layer with downstream distance. In addition to providing a number of results complementary to those for a single uniform canopy (e.g. on mean velocity profiles and turbulent shear stress), we present new data on turbulence and intermittency that confirm the prominent role of coherent structures in canopy flow.

The remainder of the paper is organised as follows. In Sect. 2, we describe the experimental laboratory apparatus and the techniques of measurement. Results on measurements

of boundary-layer characteristics are shown and discussed in Sect. 3. Finally, concluding remarks are given in Sect. 4.

2 Experimental Design

2.1 Model Description

Experiments were carried out in a water flume at the University of Delaware's Ocean Engineering Laboratory. Two hypothetical crop canopies were constructed within the water flume, and their effects on turbulent flow were measured.

The choice of a water flume is essentially motivated by practical considerations. Since the kinematic viscosity of water is less than that of air, similar Reynolds numbers can be achieved in water flumes for canopy size and flow speed smaller than in wind tunnels. As an indication, a Reynolds number (Re) in our experiments is given by Re $= 23{,}000$ (with a free-stream velocity $U_\infty = 0.092\,\mathrm{m\,s^{-1}}$ and an internal boundary-layer thickness $\delta_c \approx 0.25\,\mathrm{m}$). Besides practical considerations, we also expect the present water-flume study to be of relevance to canopy flows in environmental aquatic systems that, as shown in Ghisalberti and Nepf (2006), share many common features with their atmospheric analogues (see also Peterson et al. 2004; Folkard 2005; Poggi et al. 2007).

The water flume is built of plexi-glass and its dimensions are 0.4 m high, 0.25 m wide and 3 m long. A 0.013 m tall barrier along with a 0.1 m tall vortex generator system were positioned upstream of the two canopies. Their role was to rapidly diffuse vorticity to generate a sufficiently deep turbulent layer over the working section (Counihan 1969). In this paper, we restrict our attention to turbulent flow caused by two-dimensional variations in surface roughness. The x-axis is the main axis of the water flume, positive in the flow direction; the z-axis is vertical, normal to the water-flume floor and oriented upwards. The vortex generator system is located at $x = 0$ and the ground surface beneath the canopy elements corresponds to $z = 0$ (Fig. 1). The upstream (lower) canopy starts at $x = 0.33\,\mathrm{m}$, and the step change between the two canopies is located at $x = 1.29\,\mathrm{m}$. The heights of the upstream and downstream canopies are $h = 0.025$ and 0.05 m respectively, so that the difference in height is $\delta h = 0.025\,\mathrm{m}$. The total length of the model canopy is 1.57 m, extending from $x = 0.33\,\mathrm{m}$ to $x = 1.9\,\mathrm{m}$. The crop structure was represented by a commercial brand of toothpicks, with a diameter of 0.001 m, and fitted into drilled holes on the face of the plexi-glass and placed in a regular lattice arrangement. The holes containing the toothpicks were 0.02 m apart in both the x- and y-directions, forming a square grid with a diagonal of 0.0283 m.

By using rigid roughness elements, we only focus on studying the effects induced by the canopy structure on the flow passing over it and do not consider effects due to mutual interactions such as coherent waving motions in the case of flexible canopies. Our model canopy with a step change in surface roughness can thus be viewed as an idealised representation of forest canopies e.g. on topography or at the edge of plantation fields. The leaf area indices (LAIs) in our experiments are 0.0625 and 0.125 for the upstream and downstream canopies respectively (a 0.001 m wide by 0.025 or 0.05 m tall element for each $0.02 \times 0.02\,\mathrm{m}^2$ square), which corresponds to relatively sparse canopies. These LAIs are an order of magnitude smaller than would typically be found in real vegetation canopies. We note however that small values of LAI, of order $O(10^{-1})$, have often been used in model experiments (e.g. Raupach et al. 1987a, b; Brunet et al. 1994; Poggi et al. 2004b). Here, sufficient spacing between the toothpicks was needed to properly position measuring probes within the canopies. The use of rigid toothpicks also prevents the interior probes from being hit as might

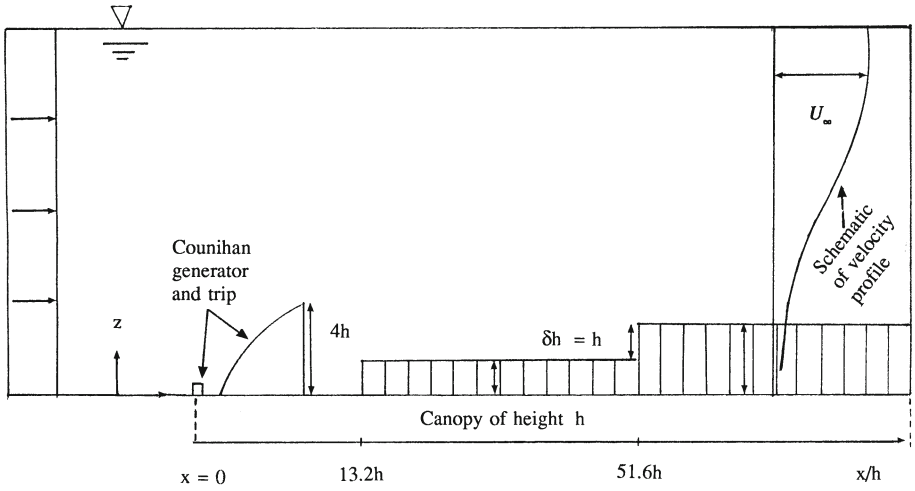

Fig. 1 Sketch of the experimental set-up. The model canopy consists of two rigid canopies of different heights ($h = 0.025$ m and 0.05 m), with the step change in surface roughness located at $x/\delta h = 51.6$ ($\delta h = 0.025$ m). A vortex generator system is positioned upstream of the model canopy

occur in the case of flexible roughness elements, and gives us a well-defined constant height for each of the canopies. As will be shown in Figs. 3 and 9, the choice of the model was examined by comparison with numerical and field data; a reasonably good agreement was found.

We also note that the limited width of the flume has implications on the size of the biggest eddies generated by the canopy, and the secondary boundary layer that develops on the sides of the flume can grow over such long distances so as to affect the canopy flow downstream. However, in the present set-up, for measurements along the main central axis of the flume and for distances up to $x = 1.8$ m $= 72\,\delta h$, we did not observe any significant effect of this secondary boundary layer.

2.2 Measurement Techniques

Flow velocities were measured with a hot-film anemometer that was calibrated against a flow manometer. The free-stream speed was constant throughout the experiments, $U_\infty = 0.092\,\mathrm{m\,s^{-1}}$, and served as a reference for the velocity measurements. To make sure that it remained constant along the water flume, we checked the value of the mean horizontal velocity above the boundary layer by dropping dye streaks (from potassium permanganate crystals) and measuring their speed between the two top probes located at the extremities of the working section (see below for a description of the probe arrangement).

The mean velocity within and above the canopies was measured with an AN-1003 hot-film anemometry system (manufactured by A.A. Lab Systems Ltd). Two-component TSI '20W' hot-film probes were employed, and sensors were arranged orthogonally, allowing us to measure velocities in two perpendicular directions simultaneously. The sensor resistances were 5.27 and 5.05 ohms. Calibration was performed by using a constant flow through a nozzle (≈ 0.02 m in diameter), the sensors being placed inside the nozzle, and calibration curves were determined for each hot film by measuring voltages for known flow speeds. It is essential that the hot films be accurately calibrated, especially for relatively low speeds

within the canopy structure. Both regimes of laminar and turbulent flows were tested, and the experiments were conducted under near-neutral stability conditions.

Data are presented here in dimensionless form. Mean velocities are normalised in two ways: either by the free-stream speed (U_∞) or by the mean horizontal flow speed at canopy height ($\overline{u}_h$ which depends on the horizontal location of the probe). Lengths are normalised by either the difference in canopy height ($\delta h = 0.025\,\mathrm{m}$) or by the actual canopy heights. Hereinafter, the height h corresponds to $h = 0.025\,\mathrm{m}$ when referred to the upstream canopy and to $h = 0.05\,\mathrm{m}$ when referred to the downstream canopy. The symbol $\overline{()}$ denotes mean quantities that are determined by time averaging over a period of 30 s.

3 Experimental Results

3.1 Mean Flow Characteristics

Mean horizontal and vertical flow speeds $\overline{u}$ and $\overline{w}$ were measured at eight stations located at $x/\delta h = 24, 36, 44, 48, 53, 56, 60, 72$ along the main central axis of the model canopy; the step change being located at $x/\delta h = 51.6$ (Fig. 1). Each station consists of an array of probes placed at various heights within and above the canopies: starting at $z = 0.01\,\mathrm{m}$ and thereafter at every 0.01 m up to $z = 0.06\,\mathrm{m}$; then at every 0.02 m up to $z = 0.1\,\mathrm{m}$, and finally at every 0.05 m up to $z = 0.25\,\mathrm{m}$ (the total water depth was 0.3 m).

We acknowledge that a larger number of probes more densely distributed in both the horizontal and vertical directions would be necessary for a finer spatial resolution of data. The present probe arrangement was found to be a sufficiently good compromise, given the experimental resources available at the time when the experiments were carried out. For graphical purposes, we used cubic interpolation to estimate the values between the probes in the plots of the mean velocity profiles (we also did so for the turbulence intensity and shear stress profiles).

As will be shown below, the internal boundary layer above the canopy resembles a smooth-to-rough transition according to internal boundary-layer depth considerations. However, beyond the thickness of this internal boundary layer, the differences remain fundamental, especially inside the canopy (no analogue in the smooth-to-rough experiments).

3.1.1 Growth of the Internal Boundary Layer

The thickness of the internal boundary layer δ_c was defined as the height at which the horizontal mean velocity $\overline{u}$ attains 99% of the free-stream value U_∞ (Garratt 1990). Figure 2 plots our measurements of δ_c as a function of x, along with the power-law approximation

$$\frac{\delta_c}{z_{01}} = \alpha \left(\frac{x}{z_{01}} \right)^{\beta}, \tag{1}$$

for a turbulent boundary layer over a flat plate, where $\alpha = 0.75 + 0.03\,\ln(z_{02}/z_{01})$ and $\beta = 4/5 = 0.8$ in neutral conditions (Panofsky and Dutton 1984; Arya 1988). Here $z_{01} = 0.35 \times 10^{-3}\,\mathrm{m}$ and $z_{02} = 1.418 \times 10^{-3}\,\mathrm{m}$ are the estimated roughness lengths for the upstream and downstream canopies, respectively. Observations of turbulent flow from smooth to rough surfaces in the atmosphere are generally consistent with the turbulent boundary-layer growth over a smooth plate, i.e. $\delta_c \propto x^{4/5}$ (Antonia and Luxton 1971; Garratt 1990).

Our measurements seem to fit more closely to an $x^{1/2}$ dependence over the range $x/\delta h =$ 24–72, a difference with (1) that can be attributed to the Counihan vortex generator, located

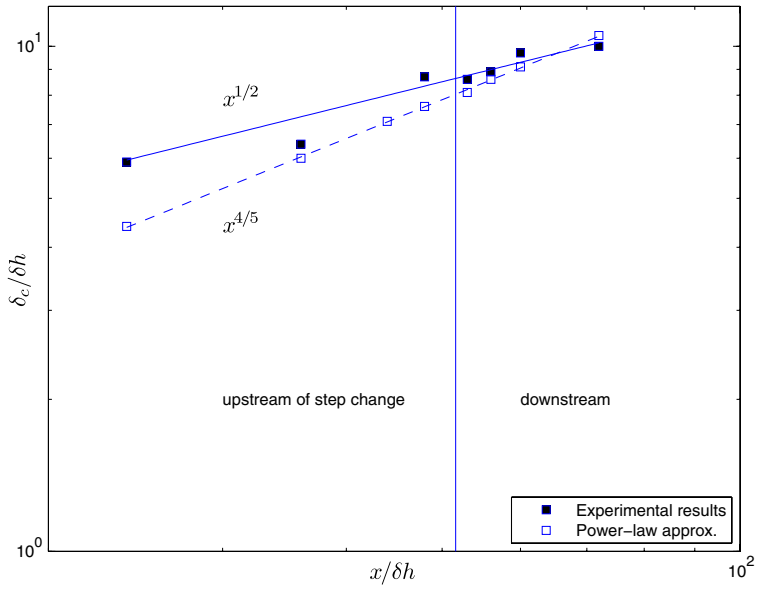

Fig. 2 Thickness of the internal boundary layer δ_c as a function of downstream distance x. The power-law approximation $\delta_c/z_{01} = \alpha\,(x/z_{01})^{4/5}$ (Eq. 1) is also plotted

at $x = 0$, which sets the initial scale of the boundary layer. Indeed, as suggested in Fig. 2, the largest discrepancy between measured and predicted values occurs for $x/\delta h = 24$ (at the most upstream station). The vortex generator was used to quickly diffuse turbulence and thicken the incoming boundary layer at the beginning of the working section, and explaining why the measured value of δ_c at $x/\delta h = 24$ is significantly larger than that predicted by (1). We see that the observations are fairly scattered upstream of the step change but, in the downstream part, they tend to be closer to the predicted slope. This suggests that, far away from the vortex generator, the growth of the internal boundary layer tends to relax to an $x^{4/5}$ profile. In this regard, the present case of turbulent flow from a rough to rougher surface appears to be similar to that for a smooth-to-rough transition.

3.1.2 Mean Velocities

Vertical profiles of the normalised mean horizontal flow speed $\overline{u}/\overline{u}_h$ for various downstream locations are depicted in Fig. 3. Upstream of the step change, the perturbations are rather weak but we can see a tendency to inflection around the canopy height $z = h$. As we move down to the rougher canopy, the shape of the inflection region becomes more pronounced and its magnitude becomes larger (Fig. 3). A similar difference in the mean velocity profiles was observed by Poggi et al. (2004b) when comparing sparse and dense canopies. Our observations are consistent with the common mixing-layer picture for canopy flow, in which an inflection point occurs at canopy height. This inflection is a necessary condition for the occurrence of Kelvin–Helmholtz instability.

Careful examination however indicates that, instead of a smooth single inflection, the velocity profiles at $x/\delta h = 53, 60, 72$ show a more perturbed picture. A localised perturbation in the inflection region persists far beyond the step change, and tends to move from $z/h = 0.5$ (height of the upstream canopy) at $x/\delta h = 53$ to $z/h = 1$ (height of the

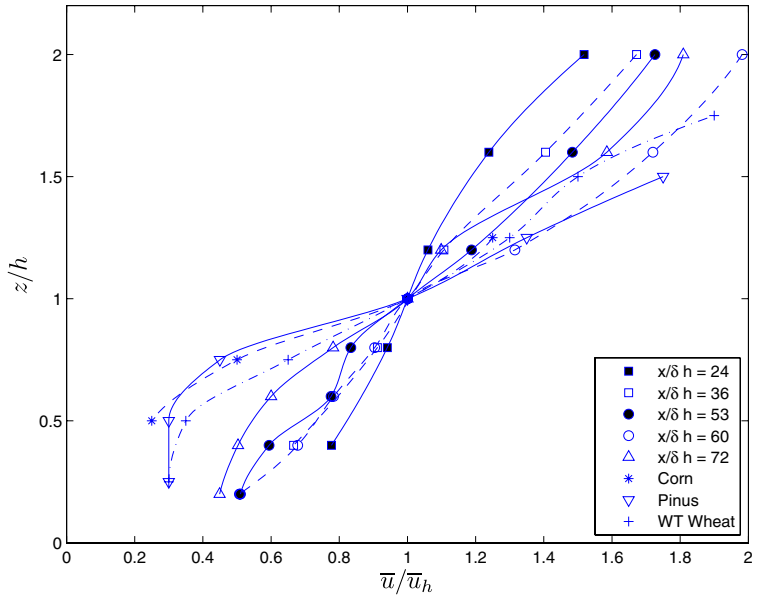

Fig. 3 Vertical profiles of mean horizontal flow speed normalised by the mean horizontal speed at canopy height, within and above the canopy as well as upstream ($h = 0.025$ m) and downstream ($h = 0.05$ m) of the step change. Observations from a cornfield and a plantation of Pinus as well as from a wheat canopy model in a wind tunnel are also plotted

downstream canopy) at $x/\delta h = 72$. This suggests that the perturbation may be due to residual shear produced by the lower canopy that adds to the shear by the taller canopy. The turbulent flow in the present configuration is therefore a more perturbed mixing layer than in the case of a single uniform canopy.

Figure 3 also shows a comparison of our water-flume experiments with field data from a cornfield (Shaw et al. 1974a) and a plantation of Pinus (Y. Brunet, personal communication, 2008; see also Kaimal and Finnigan 1994), as well as with data from a wheat canopy model in a wind tunnel (Brunet et al. 1994). Despite the differences in scales and foliage types, general similarities are observed between the water-flume and atmospheric results. The emerging pattern here is very similar to that reported in Morse et al. (2002), where wind-tunnel experiments were performed to investigate the transition from a short canopy (open moorland) to a forest canopy. In accordance with our results, these authors observed a strong shear as the flow passes the forest edge. They also observed an adjustment of turbulence intensities and shear stress to the forest canopy, which is similar to the present situation for a flow passing a step change in surface roughness (see Sects. 3.2, 3.4).

Examination of the mean horizontal velocity at isoheights along the canopies indicates that the strongest variations occur above the canopies, in the region near the step change (Fig. 4). Far within and above the canopies, as well as away (upstream and downstream) from the step change, the perturbations are less dramatic. A strong acceleration followed by an equally strong deceleration occurs in the upstream vicinity of the step change, for $z/\delta h \geq 1.2$. Within the canopy ($z/\delta h = 0.4$), the picture seems to be reversed (deceleration and then acceleration between $x/\delta h = 44$ and 53), but in smaller proportions.

The mean vertical velocities (not shown here) are typically two orders of magnitude smaller than their horizontal analogues. They change little either in the horizontal or vertical

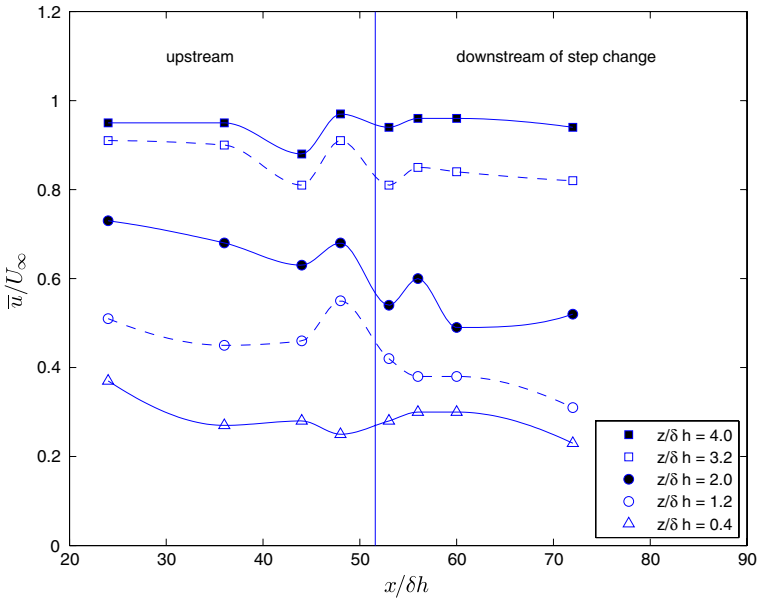

Fig. 4 Profiles of mean horizontal flow speed along isoheights, within and above the canopy. The vertical line represents the location of the step change at $x/\delta h = 51.6$

direction. Normalised values $\overline{w}/U_\infty$ range from -0.03 to 0.05 approximately: positive values are mostly observed around and below the canopy tops, while negative values occur above the canopies.

3.2 Turbulence Intensities

Horizontal and vertical turbulence intensities

$$\frac{\sigma_u}{U_\infty} = \frac{\sqrt{\overline{u'^2}}}{U_\infty}, \tag{2a}$$

$$\frac{\sigma_w}{U_\infty} = \frac{\sqrt{\overline{w'^2}}}{U_\infty}, \tag{2b}$$

(i.e. standard deviations normalised by free-stream speed) were calculated at two stations located upstream of the step change ($x/\delta h = 24, 36$), and at three stations downstream ($x/\delta h = 53, 60, 72$). Here u' and w' denote the turbulent fluctuations in u and w respectively.

Their vertical distributions at these different locations are presented in Fig. 5. A general observation is that σ_u and σ_w are of the same order of magnitude, unlike the mean velocities, and their profiles almost coincide and are quasi-uniform with height at the upstream locations. However, past the step change, they exhibit more variations and relative differences: σ_w tends to be slightly smaller than σ_u but both intensities seem to peak at canopy height (this similarity between σ_u and σ_w will be discussed further in Sect. 3.4, when analysing the shear stress).

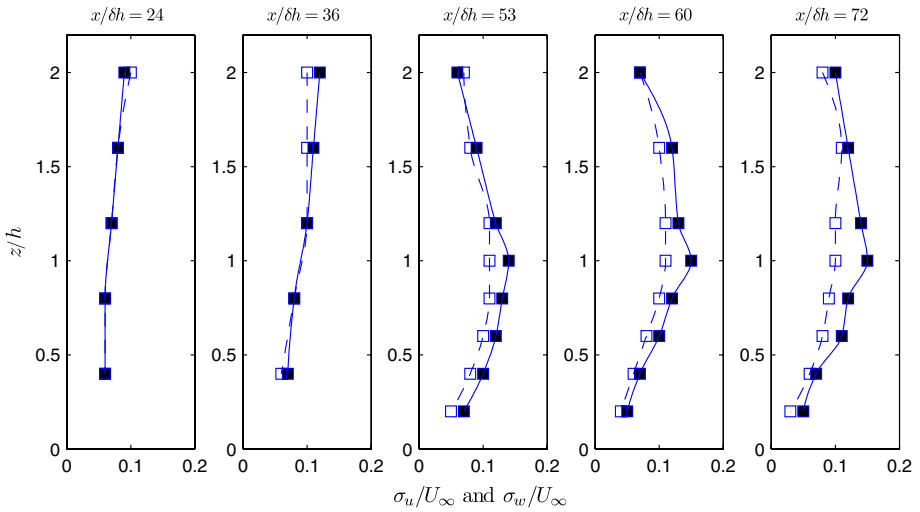

Fig. 5 Vertical profiles of horizontal (solid line) and vertical (dashed line) turbulence intensities, at $x/\delta h = 24$, 36 (upstream) and $x/\delta h = 53$, 60, 72 (downstream of the step change)

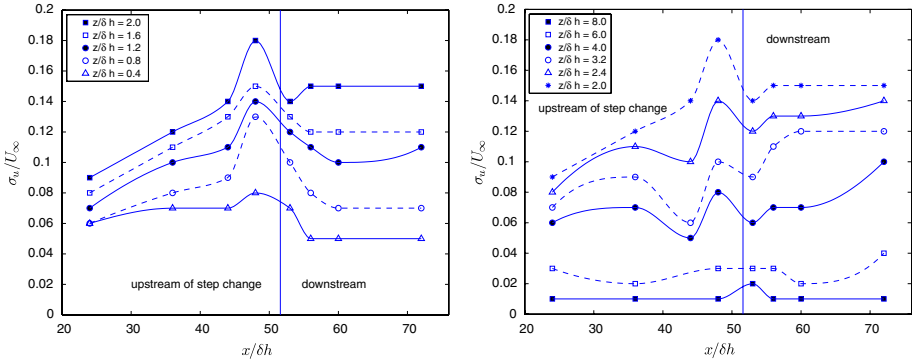

Fig. 6 Profiles of horizontal turbulence intensity along isoheights, within and just above the canopy (left) and far above the canopy (right)

As an indication, the two upstream stations show horizontal intensity maxima of 9% and 12% (of free-stream speed), while the downstream stations record maxima of 14%, 15% and 15%, respectively. Isoheights of horizontal intensities reveal that the largest variations occur in the upstream vicinity of the step change, between $z/\delta h = 2$ and 4 above the canopy (Fig. 6). These large variations consist of an increase followed by a decrease, and such a similarity with the observations in Fig. 4 indicates some correlation between σ_u and $\overline{u}$. As the flow approaches the taller canopy, it is accelerated and then decelerated due to the pressure gradient caused by the roughness change, creating turbulence that follows the same pattern and diffuses away vertically. Diffusion is strong near the step change because the turbulence intensity and pressure gradient are large there (Cassiani et al. 2008). A similar behaviour is observed for σ_w in Fig. 7, which is consistent with the distribution of σ_w showing peak values at canopy height in Fig. 5. For comparison, vertical turbulence intensities reach a maximum of 11% (of free-stream speed) at the downstream locations.

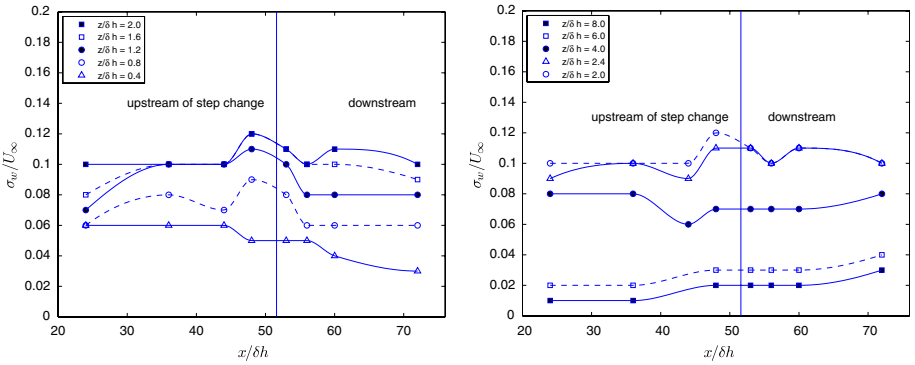

Fig. 7 Profiles of vertical turbulence intensity along isoheights, within and just above the canopy (left) and far above the canopy (right)

Our results show that abrupt changes in surface roughness can be an important source for turbulence generation in canopy flows.

3.3 Turbulence Spectra

Frequency power spectra of horizontal and vertical turbulent velocities, $S_u(f)$ and $S_w(f)$, were also measured. Results for heights $z/h = 0.6, 1$ at the downstream station $x/\delta h = 72$ are presented in Fig. 8, though we obtained similar spectra at the other stations and at other heights. Here spectral characteristics do not vary much with the location, either horizontally (i.e. upstream or downstream of the step change) or vertically (i.e. within or above the canopy).

Figure 8a and c depict the horizontal power spectra at $z/h = 0.6$ and 1 respectively, while Fig. 8b and d portray the corresponding vertical spectra, all plotted against the dimensionless frequency $f\,h/\overline{u}_h$. This scaling is motivated by that used for the atmospheric surface layer $n = f\,(z - d_0)/\overline{u}$ where d_0 denotes the displacement height (Shaw et al. 1974b; Brunet et al. 1994). Previous studies found that the peak frequency, which provides an inverse time scale for the energy-containing eddies, tends to be independent of height. This feature is also observed here; all four spectra in Fig. 8 exhibit a high-energy region around $f\,h/\overline{u}_h = 0.2$ that is close to the values reported in e.g. Brunet et al. (1994) and Finnigan (2000). Here, 0.2 can be viewed as the typical Strouhal number associated with large vortices (coherent structures) of size $O(h)$ shed from the canopy structure.

Regarding the spectral shapes, we see that all four spectra compare well with Kolmogorov's $-5/3$ law over an inertial range of about one decade. In doing so, we assume Taylor's 'frozen turbulence' hypothesis to transcribe Kolmogorov's law into the frequency domain. The agreement is especially good for the vertical spectrum at both $z/h = 0.6, 1$; the horizontal spectrum however tends to roll off more slowly than $-5/3$ at high frequencies as we descend into the canopy (Fig. 8a). This difference between the horizontal and vertical spectra is related to the lack of isotropy within the model canopy, especially in the horizontal direction due to the toothpick arrangement. Isotropy would imply that $S_w(f)/S_u(f) = 4/3$ (see Hsieh and Katul 1997 for a detailed discussion on how to correct this ratio for distortions arising from Taylor's hypothesis).

As discussed in Finnigan (2000), the deviation from Kolmogorov's theory, observed here for $S_u(f)$ within the canopy, may be attributed to, (i) work by the mean flow against the

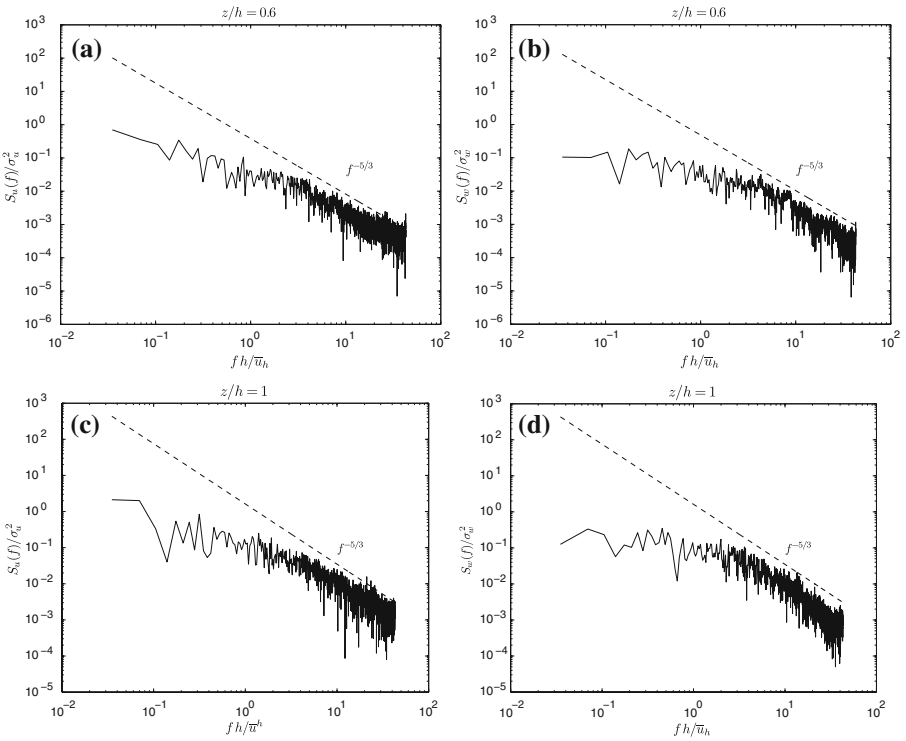

Fig. 8 Frequency power spectra at the downstream station $x/\delta h = 72$, within ($z/h = 0.6$) and at the top ($z/h = 1$) of the canopy. Panels (**a**) and (**c**) show the horizontal spectra, while panels (**b**) and (**d**) show the vertical spectra

foliage drag, producing fine-scale turbulence in the wakes of canopy elements, and (ii) the spectral short-circuiting of the energy cascade, which represents the same physical process as described in (i) but acting on turbulent eddies rather than the mean flow. These two processes lead to fast transfer of energy from large to small scales, in contradiction with the classical picture of energy cascade in Kolmogorov's theory, and may explain the small energy pile-up at high frequencies in Fig. 8a. Experimental data in support of this theory can also be found in Poggi et al. (2004b).

Taylor's hypothesis is justified in our experiments by the fact that both turbulent velocities u' and w' are typically much smaller than the mean horizontal speed $\overline{u}$. The overall good agreement between the measured spectra and Kolmogorov's theory further confirms the validity of this hypothesis.

3.4 Shear Stress

Vertical profiles of the Reynolds shear stress normalised by the friction velocity ($-\overline{u'w'}/u_*^2$) are shown in Fig. 9 for the stations located at $x/\delta h = 24, 36, 53, 60, 72$.

Each profile depicts a maximum near the canopy top, with a trend to decrease both above and below $z/h = 1$. There are nevertheless some notable differences depending on the station's location. At the first station of each canopy ($x/\delta h = 24$ and 53), we observe a zone of almost constant shear stress above $z/h = 1$, in accordance with Brunet et al. (1994). As we

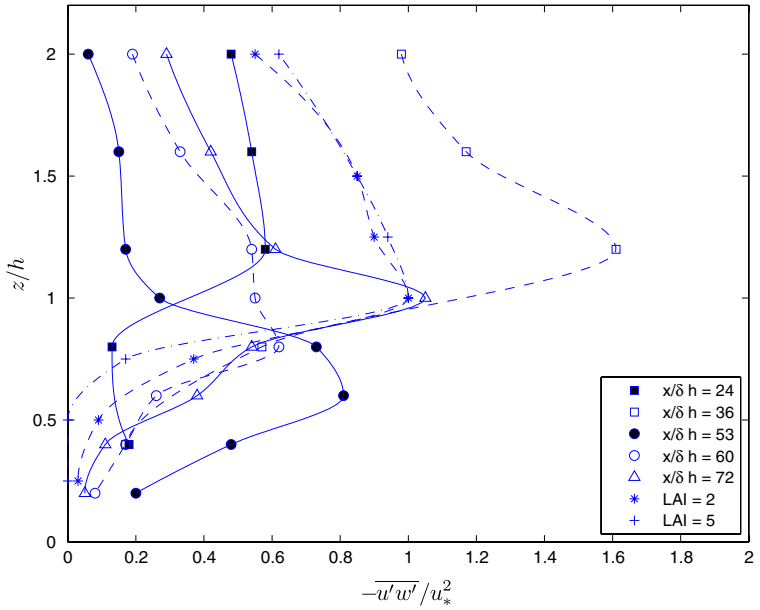

Fig. 9 Vertical profiles of Reynolds shear stress (normalised by friction velocity u_*), upstream and downstream of the step change. Data from large-eddy simulations for LAI = 2, 5 (Shaw and Schumann 1992) are also plotted

go further down the canopies, however, the shear stress increases and its profile converges to a characteristic cusp-like shape centred at $z/h = 1$, consistent with the observations of e.g. Poggi et al. (2004b); Ghisalberti and Nepf (2006), and Zhu et al. (2006). Maximum shear stress coincides with maximum turbulence at canopy height, as indicated in Fig. 5. The turbulence produced in this region is thus most efficient in transferring momentum. Results from large-eddy simulations for LAI = 2, 5 by Shaw and Schumann (1992) are also presented in Fig. 9. While these results were obtained for uniform canopies, they compare qualitatively well with our experimental data, in particular regarding the location and magnitude of the peak value.

Closer examination of the profiles at $x/\delta h = 53, 60, 72$ (past the step change) also reveals that the shear stress tends to adjust to the taller canopy, its peak moving from $z/h = 0.5$ to $z/h = 1$. This adjustment of the shear stress is consistent with that of the mean horizontal velocity, as discussed earlier (Fig. 3).

Similar observations can be made when examining the correlation coefficient $r_{uw} = -\overline{u'w'}/(\sigma_u \sigma_w)$, which gives a measure of the shared variance between horizontal and vertical turbulence (not shown here). In particular, we found that r_{uw} at $x/\delta h = 24$ above $z/h = 1$ takes an almost constant value of about 0.31, which is very close to Brunet et al.'s (1994) value of 0.35.

Shear stress decreases with decreasing height but also with downstream distance. Values of the downstream shear stress τ_{02} at $z/h = 0.2$ ($z = 0.01$ m), normalised by a reference upstream value τ_{01} (chosen at $x/\delta h = 24$ and $z/h = 0.4$), are given by $\tau_{02}/\tau_{01} = 2.65, 1.43, 1.02, 0.82$ for $x/\delta h = 53, 56, 60, 72$ respectively. The reason for considering τ_{01} and τ_{02} at $z = 0.01$ m is that the shear stress is almost constant along the upstream canopy at this height (Fig. 9). We see that τ_{02}/τ_{01} decreases rapidly from 2.65

at $x/\delta h = 53$ to an equilibrium value of about 0.82 at $x/\delta h = 72$. Most of the shear stress variation occurs immediately behind the step change between $x/\delta h = 51.6$ and 60.

This relaxation to equilibrium by a factor of ≈ 0.31 (ratio of 0.82 to 2.65) is consistent with the observations of Bradley (1968); Rao et al. (1974) and Belcher et al. (1990), who found maximum stresses of 8.0 and an equilibrium value of about 3.0 for a smooth-to-rough transition, corresponding to a decrease by a factor of ≈ 0.37. We point out again that τ_{01} and τ_{02} were measured at the same height $z = 0.01$ m near the ground surface, so τ_{02} is expected to be smaller than τ_{01} since the downstream canopy is taller, and thus the corresponding stress generated at canopy height decreases further with decreasing z.

This shear stress decay may be explained as follows. The fluid above the upstream canopy flows fairly rapidly when it encounters the abrupt change in surface roughness. As the fluid encounters the rougher surface, it decelerates because of increased surface friction. This deceleration, which is initially confined to the fluid layers in contact with the new surface, is diffused vertically by turbulence. As the new rougher surface absorbs momentum from the fluid layers above, this region of decelerated flow thickens. The speed of the fluid layers in contact with the enhanced roughness decreases and so does the resulting surface stress.

The focus here is on quantifying the Reynolds shear stress. However we note that dispersive stresses can also be a non-negligible contribution to momentum transfer in sparse canopies because of their large spatial variability. Poggi et al. (2004a) showed that the dispersive stresses occurring in such canopies can be as much as 30% in magnitude of the Reynolds shear stress. It would be of interest to investigate in detail their role in the present model canopy using a non-intrusive, higher-precision measuring system.

3.5 Intermittent Events

Intermittency in canopy turbulence arises from essentially two mechanisms: shear within and at the top of the canopy, and vortex shedding within the canopy. The former is responsible for the emergence of large coherent structures induced by Kelvin–Helmholtz instability at canopy height (see Sect. 3.1). The latter mechanism is associated with wake production (the so-called von Kármán vortex streets) behind individual canopy elements, which may contribute to the departure from Kolmogorov's theory in the horizontal power spectrum (see Sect. 3.3).

One way to further quantify intermittency in canopy flow is to examine the time series and magnitude of instantaneous shear stress $u'w'$. Time series analysis allows us to determine the frequency of occurrence of extreme intermittent uw events, which can be used as a measure of shear effects.

The frequency of intermittent events was determined in the following manner. Given a time series of 30 s recorded at a probe, the number of large uw events was estimated based on an empirical threshold, i.e. all $|u'w'| > e^{-1}|u'w'|_{\max}$ where $|u'w'|_{\max}$ denotes the largest value in the time series record (Fig. 10). The number of peak values exceeding this threshold divided by the time series duration (30 s) then gives the frequency of intermittent events, f. The choice of the factor e^{-1} is empirical and is motivated by the exponential-like decaying profiles of the mean horizontal velocity and Reynolds shear stress within the canopy (see Figs. 3 and 9).

Intermittent events associated with shear can be quantified based on the non-dimensional frequency $f/(\partial\overline{u}/\partial z)$, and Fig. 11 plots $f/(\partial\overline{u}/\partial z)$ as a function of z/h, obtained from our experiments. Three sets of data are shown for the stations at $x/\delta h = 36$ (upstream) and

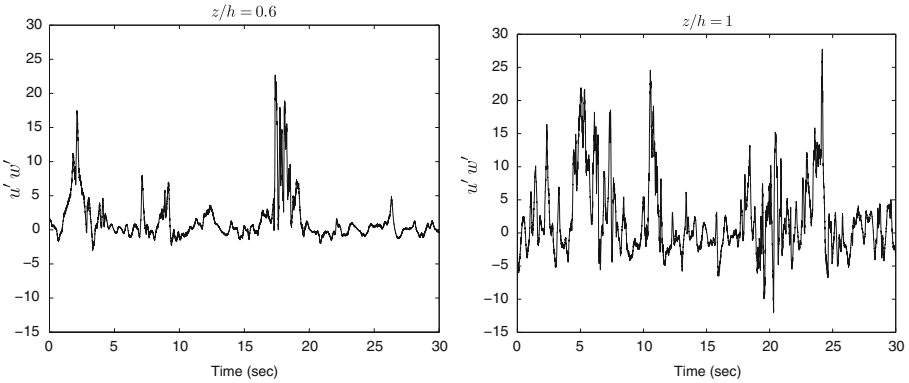

Fig. 10 Instantaneous shear stress $u'w'$ at $x/\delta h = 72$ (downstream of the step change), within and at the top of the canopy ($z/h = 0.6, 1$)

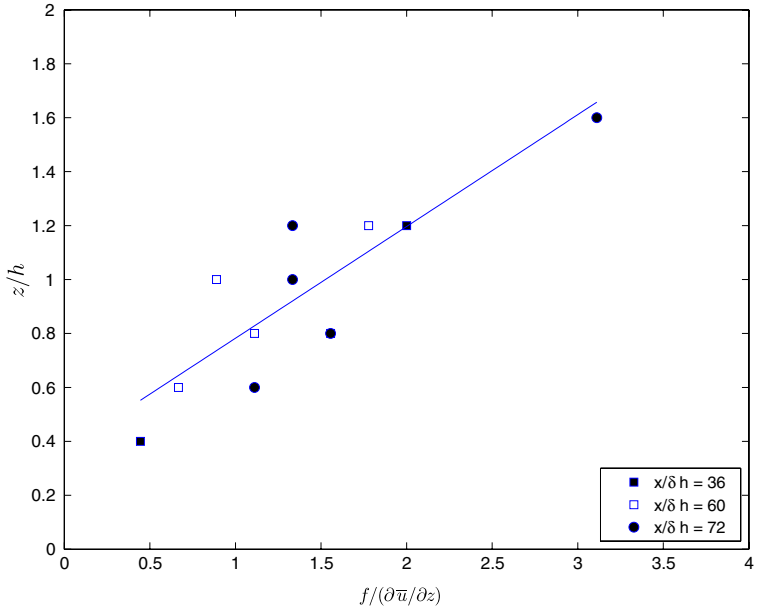

Fig. 11 Vertical frequency distribution of instantaneous uw events, at $x/\delta h = 36$ (upstream) and $x/\delta h = 60, 72$ (downstream of the step change). The straight line represents a linear fit to the three datasets. Note that $\partial\overline{u}/\partial z = 0.45\,\mathrm{s}^{-1}$ is taken from Fig. 3

$x/\delta h = 60, 72$ (downstream of the step change). Our results are fairly dependent on height and indicate that $0 < f/(\partial\overline{u}/\partial z) < 3$; values of order $O(10^{-1})$ were found for $z/h < 0.5$, while values of order $O(1)$ were obtained in the upper part of the model canopy. Figure 11 suggests that $f/(\partial\overline{u}/\partial z)$ increases about linearly with height, at least up to $z/h \approx 1.2$. This increase is consistent with the vertical profiles of turbulence intensities in Fig. 5 and of Reynolds shear stress in Fig. 9, and is further evidence of large coherent structures occurring at canopy height.

The relative importance of shear and vortex shedding can be assessed by comparing the Strouhal number (St) associated with large vortices produced by the canopy structure

$$\mathrm{St} = f\frac{h}{\overline{u}_h}, \tag{3}$$

and that associated with smaller vortices shed from individual canopy elements

$$\mathrm{St} = f^*\frac{d}{\overline{u}_h}, \tag{4}$$

where $d = 0.001\,\mathrm{m}$ is the diameter of the canopy elements; St is typically equal to 0.2. Equating (3) and (4), we obtain

$$\frac{f}{f^*} = \frac{d}{h}. \tag{5}$$

If $f/f^* \approx 1$, intermittency induced by vortex shedding will tend to be as important as shear-induced intermittency, within the canopy. Here we have $f/f^* = 0.04$ and 0.02 ($\ll 1$) for the upstream and downstream canopies respectively, which suggests that shear is the dominant mechanism of intermittency for $z/h < 1$. Another indication that vortex shedding is of lesser importance here is the relatively small departure from Kolmogorov's theory, as shown in Fig. 8. Moreover, the spectra apparently exhibit no secondary peak at $f\,h/\overline{u}_h \approx 10$, which would correspond to the typical Strouhal number $\mathrm{St} = f\,d/\overline{u}_h = 0.2$ for vortex shedding behind individual canopy elements (Poggi et al. 2004b; Poggi and Katul 2006; Cava and Katul 2008).

Note that intermittency of uw events is also likely to be dependent on LAI (i.e. on canopy density). Kaimal and Finnigan (1994) showed that, in dense canopies (LAI > 1), most of the momentum is absorbed in the upper zone ($z/h \approx 1$) so that the shear stress transmitted to the ground surface is essentially zero. In the present experiments, the LAI is relatively small (LAI $= 0.0625$ and 0.125 for the upstream and downstream canopies respectively), and we observe that both the mean horizontal velocity and shear stress persist throughout the depth of the model canopy, down to near the bottom (Figs. 3 and 9). This supports the conclusion that the dominant mechanism of momentum transfer, as indicated by uw intermittency, is likely to be shear.

4 Conclusions

Water-flume experiments have been conducted to study the structure of turbulent flow within and above a sparse model canopy consisting of two rigid canopies of different heights. This difference in height specifies a two-dimensional step change from a rough to a rougher surface, as opposed to a smooth-to-rough transition. The structure of the turbulent velocity field as well as the evolution and geometry of the boundary layer have been investigated in detail through measurements of various boundary-layer characteristics.

Overall, the results are consistent with the classical picture of canopy turbulence for a smooth-to-rough transition, in particular regarding the vertical profiles of mean horizontal velocity and shear stress. However there are notable differences, specific to the present situation. New results on turbulence and intermittency are obtained, supporting the prominent role of large coherent structures in canopy flow.

Vertical profiles of mean horizontal velocity past the step change exhibit a perturbed inflection zone, which tends to move from $z/h = 0.5$ to $z/h = 1$ as we go further downstream.

This adjustment to the downstream (taller) canopy is also reflected in the vertical profiles of shear stress.

Changes in velocity are larger in the vicinity of the step change and the canopy top. In particular, a large horizontal acceleration followed by an equally large deceleration is observed in the upstream vicinity of the step change, above the model canopy. Large variations in horizontal turbulence intensity tend to coincide with large variations in mean horizontal velocity. Horizontal and vertical turbulence intensities are found to vary in the same manner with downstream distance and height. The effects of the step change are felt up to almost $z/\delta h = 5$.

Horizontal and vertical turbulence spectra, within and above the canopy, agree well with Kolmogorov's theory, although some small energy pile-up at high frequencies is detected in the horizontal spectrum. This phenomenon is especially apparent within the canopy, and may result from fast transfer of energy from large to small scales due to wake production and work by the mean flow against form drag.

Shear stress and correlation coefficient tend to peak at canopy height, both upstream and downstream of the step change. Above and below this height, they decrease monotonically. Past the step change, the shear stress rapidly decreases with downstream distance to relax to an equilibrium value. This relaxation to equilibrium occurs only within a distance of $\approx 10\,\delta h$ from the step change.

Analysis of uw intermittency points to shear as the dominant mechanism for momentum and turbulence generation within the present model canopy, as compared to vortex shedding from individual canopy elements. The frequency of instantaneous uw events is found to increase about linearly with height. Mean velocity profiles also show that shear is responsible for the development of large coherent structures at canopy height and, here for relatively low LAI, shear persists deep within the canopy.

The thickness of the internal boundary layer is found to grow approximately like $x^{4/5}$ with distance x downstream of the step change, which is similar to the situation for a turbulent boundary layer over a smooth plate.

Finally, we acknowledge that better-resolved measurements (using e.g. laser Doppler anemometry, particle image velocimetry) are called for to supplement the present results. It would also be of interest to examine the effects of canopy density (in the presence of a step change in surface roughness) on the turbulence structure, as well as three-dimensional effects. These directions of inquiry are envisioned for future work.

Acknowledgements The authors gratefully acknowledge advice and assistance from Dan Leathers, Pablo Huq for his help with the experiments, and the University of Delaware's Ocean Engineering Laboratory where the experiments were carried out. P. Guyenne gratefully acknowledges support from the University of Delaware Research Foundation and the National Science Foundation through grant No. DMS-0625931.

References

Antonia RA, Luxton RE (1971) The response of a turbulent boundary layer to a step change in surface roughness. Part I. Smooth to rough. J Fluid Mech 48:721–761

Arya SPS (1988) Introduction to micrometeorology. Academic Press, New York, 307 pp

Belcher SE, Xu DP, Hunt JCR (1990) The response of a turbulent boundary layer to arbitrarily distributed two-dimensional roughness changes. Quart J Roy Meteorol Soc 116:611–635

Belcher SE, Jerram N, Hunt JCR (2003) Adjustment of a turbulent boundary layer to a canopy of roughness elements. J Fluid Mech 488:369–398

Bergen JD (1975) Air movement in a forest clearing as indicated by smoke drift. Agric Meteorol 15:165–179

Bradley EF (1968) A micrometeorological study of velocity profiles and surface drag in the region modified by a change in surface roughness. Quart J Roy Meteorol Soc 94:361–379
Brunet Y, Finnigan JJ, Raupach MR (1994) A wind tunnel study of air flow in waving wheat: single-point velocity statistics. Boundary-Layer Meteorol 70:95–132
Cassiani M, Katul GG, Albertson JD (2008) The effects of canopy leaf area index on airflow across forest edges: large-eddy simulations and analytical results. Boundary-Layer Meteorol 126:433–460
Cava D, Katul GG (2008) Spectral short-circuiting and wake production within the canopy trunk space of an Alpine hardwood forest. Boundary-Layer Meteorol 126:415–431
Counihan J (1969) An improved method of simulating an atmospheric boundary layer in a wind tunnel. Atmos Environ 3:197–214
Dupont S, Brunet Y (2008) Impact of forest edge shape on tree stability: a large-eddy simulation study. Forestry. doi: 10.1093/forestry/cpn006
Finnigan J (2000) Turbulence in plant canopies. Annu Rev Fluid Mech 32:519–571
Finnigan J, Brunet Y (1995) Turbulent airflow in forests on flat and hilly terrain. In: Coutts MP, Grace J (eds) Wind and Trees. Cambridge University Press, Cambridge, pp 3–40
Flesch TK, Wilson JD (1999) Wind and remnant tree sway in forest cutblocks. I. Measured winds in experimental cutblocks. Agric For Meteorol 93:229–242
Folkard AM (2005) Hydrodynamics of model *Posidonia oceanica* patches in shallow water. Limnol Oceanogr 50:1592–1600
Garratt JR (1990) The internal boundary layer—a review. Boundary-Layer Meteorol 50:171–203
Ghisalberti M, Nepf H (2006) The structure of the shear layer in flows over rigid and flexible canopies. Environ Fluid Mech 6:277–301
Hsieh CI, Katul GG (1997) Dissipation methods, Taylor's hypothesis, and stability correction functions in the atmospheric surface layer. J Geophys Res 102:16391–16405
Irvine MR, Gardiner BA, Hill MK (1997) The evolution of turbulence across a forest edge. Boundary-Layer Meteorol 84:467–496
Judd MJ, Raupach MR, Finnigan JJ (1996) A wind tunnel study of turbulent flow around single and multiple windbreaks. Part I: Velocity fields. Boundary-Layer Meteorol 80:127–165
Kaimal JC, Finnigan JJ (1994) Atmospheric boundary layer flows: their structure and measurement. Oxford University Press, Oxford, 289 pp
Morse AP, Gardiner BA, Marshall BJ (2002) Mechanisms controlling turbulence development across a forest edge. Boundary-Layer Meteorol 103:227–251
Panofsky HA, Dutton JA (1984) Atmospheric Turbulence: Models and Methods for Engineering applications. Wiley, New York, 397 pp
Peterson CH, Luettich RAJr, Michell F, Skilleter GA (2004) Attenuation of water flow inside seagrass canopies of differing structure. Mar Ecol Prog Ser 268:81–92
Poggi D, Katul GG (2006) Two-dimensional scalar spectra in the deeper layers of a dense and uniform model canopy. Boundary-Layer Meteorol 121:267–281
Poggi D, Katul GG, Albertson JD (2004a) A note on the contribution of dispersive fluxes to momentum transfer within canopies. Boundary-Layer Meteorol 111:615–621
Poggi D, Porporato A, Ridolfi L, Albertson JD, Katul GG (2004b) The effect of vegetation density on canopy sub-layer turbulence. Boundary-Layer Meteorol 111:565–587
Poggi D, Katul GG, Albertson JD, Ridolfi L (2007) An experimental investigation of turbulent flows over a hilly surface. Phys Fluids 19, 036601:1–12
Py C, Langre Ede , Moulia B (2006) A frequency lock-in mechanism in the interaction between wind and crop canopies. J Fluid Mech 568:425–449
Rao KS, Wyngaard JC, Cote OR (1974) The structure of two-dimensional internal boundary layer over a sudden change of surface roughness. J Atmos Sci 31:738–746
Raupach MR, Thom AS (1981) Turbulence in and above plant canopies. Annu Rev Fluid Mech 13:97–129
Raupach MR, Bradley EF, Ghadiri H (1987a) A wind tunnel investigation into the aerodynamic effects of forest clearings on the nesting of Abbot's Booby on Christmas Island. Internal Report to Australian National Parks and Wildlife Service, CSIRO Division of Environmental Mechanics
Raupach MR, Thom AS, Edwards I (1987b) A wind tunnel study of turbulent flow close to regularly arrayed rough surfaces. Boundary-Layer Meteorol 18:373–397
Raupach MR, Finnigan JJ, Brunet Y (1996) Coherent eddies and turbulence in vegetation canopies: the mixing layer analogy. Boundary-Layer Meteorol 78:351–382
Shaw RH, den Hartog G, King KM, Thurtell GW (1974a) Measurements of mean wind flow and three-dimensional turbulence within a mature corn crop. Agric Meteorol 13:419–425
Shaw RH, Silversides RH, Thurtell GW (1974b) Some observations of turbulence and turbulent transport within and above plant canopies. Boundary-Layer Meteorol 5:429–449

Shaw RH, Schumann U (1992) Large-eddy simulation of turbulent flow above and within a forest. Boundary-Layer Meteorol 61:47–64

Yang B, Morse A, Shaw RH, Paw U KT (2006a) Large-eddy simulation of turbulent flow across a forest edge. Part II: Momentum and turbulent kinetic energy budget. Boundary-Layer Meteorol 121:433–457

Yang B, Raupach MR, Shaw RH, Paw U KT, Morse A (2006b) Large-eddy simulation of turbulent flow across a forest edge. Part I: flow statistics. Boundary-Layer Meteorol 120:377–412

Zhu W, van Hout R, Luznik L, Kang HS, Katz J, Meneveau C (2006) A comparison of PIV measurements of canopy turbulence performed in the field and in a wind tunnel model. Exp Fluids 41:309–318